Astron. Astrophys. 299, 715–723 (1995)

ASTRONOMY AND ASTROPHYSICS

Late-time Hα emission from the hydrogen shell of SN 1993J*

F. Patat[1,2], N. Chugai[3], and P.A. Mazzali[4,2]

[1] Dipartimento di Astronomia, Universitá di Padova, vicolo dell'Osservatorio 5, I-35122 Padova, Italy
[2] European Southern Observatory, Karl-Schwarzschild St. 2, D-85748 Garching b. München, Germany
[3] Institute of Astronomy, Russian Academy of Sciences, Pyatnitskaya 48, 109017 Moscow, Russia
[4] Osservatorio Astronomico, Via G.B. Tiepolo, 11, I-34131 Trieste, Italy

Received 3 November 1994 / Accepted 21 December 1994

Abstract. We analyse the Hα emission line in the late time spectra of the type II–Ib SN 1993J at epochs 0.5–1 year after the explosion. The observed Hα profile is fitted assuming that ionized hydrogen is distributed in a shell with H^+ density maximum at 8900–9300 km s^{-1}, inner edge at about 7500 km s^{-1} and outer edge at about 11400 km s^{-1}. These velocities remained constant for over 6 months. The mass of H^+ in the shell required for the Hα emission to be reproduced by recombination is 0.05–0.2$M_\odot$. Energy deposition by the γ–rays generated by the radioactive decay of 0.075 $M_\odot$ of ^{56}Ni is insufficient to explain the observed Hα flux after an epoch about 150 d. The interaction of the ejecta with the circumstellar (CS) wind is probably the dominant energy source for the Hα luminosity at $t \geq 0.5$ yr. However, the standard model of the ejecta–wind interaction requires a mass loss rate $\dot{M} \approx 2\,10^{-5}(u/10$ km/s$)\,M_\odot$ yr^{-1}, which exceeds by approximately a factor 10 the upper limit derived from the Hα width and from the lack of profile evolution. Wind clumpiness may significantly increase the efficiency of the conversion of the luminosity produced by the ejecta–wind interaction into Hα radiation. The required average wind density would thus decrease and so would the estimated mass loss rate.

Key words: supernovae: general – supernovae: individual (SN 1993J)

1. Introduction

The bright supernova 1993J discovered on March 28.9 UT by F. Garcia (Ripero et al. 1993) in NGC 3031 (M 81) displayed early–on relatively strong Balmer lines, which suggested a SN II identification. A few weeks later the ambiguous nature of this object became clear, with the appearance of HeI lines marking the onset of a transition towards type Ib (Filippenko et al. 1993). Given this evidence, several authors suggested that the progenitor of SN 1993J was a massive star, with main sequence mass $M_{ms} \sim 12 - 16M_\odot$, which had lost almost all of its hydrogen envelope before the explosion (cf. Woosley et al. 1994). The large mass loss was most probably due to the presence of a close companion (cf. Nomoto et al. 1993).

The mass and the distribution of hydrogen in the envelope of SN 1993J are crucial parameters for the understanding of the pre–explosion history of this unusual supernova. Hydrodynamical models suggest that the mass of the residual hydrogen envelope is in the range 0.06 – 0.9 $M_\odot$ (Shigeyama et al. 1994; Utrobin 1993; Woosley et al. 1994; Bartunov et al. 1994). On the other hand, an analysis of the hydrogen lines in spectra obtained during the first 40 days after explosion led Swartz et al. (1993) to the conclusion that the hydrogen mass is only $\approx 0.04\ M_\odot$.

In this paper we study the behaviour of the emission line luminosity and of the profile of Hα in SN 1993J from shortly after maximum light until day 367, in an attempt to obtain an independent estimate of the hydrogen mass and to understand the origin of the energy supply giving rise to the late time Hα luminosity. First, we analyse the observed late time Hα profile, at epochs from 170 to 367 days after maximum, and compare it with the available late time spectra of other SNe Ib/c, in particular SN 1983N. We then estimate the parameters of the distribution of the ionized hydrogen. Then we apply the radioactive model for the production of Hα luminosity in an attempt to reproduce the observed behaviour of Hα. The failure of the radioactive model in explaining the Hα emission after day 120 forces us to consider the alternative ejecta–wind interaction mechanism for the Hα power supply. However, this model is also shown to present some problems.

2. Data and problem of identification

The optical spectra of SN 1993J used in this work are taken from the database presented by Barbon et al. (1994). The observations were made with the Boller & Chivens spectrograph mounted at the Cassegrain focus of the Asiago Observatory 1.82m telescope

Send offprint requests to: F. Patat

* Based on observations collected at Mt. Ekar (Italy).

on Mt. Ekar (Italy) from 15 September 1993 (day +171) to 30 March 1994 (day +367) (epochs refer to the time of outburst, 28 March 1993). The first spectrum of this set corresponds to the phase when the He I 6678 Å emission line, which is present in earlier spectra, has disappeared.

The nearly flat–topped profile at the Hα wavelength observed at epochs $t \geq 1$ yr and identified with Hα by Clocchiatti & Wheeler (1994) is clearly detectable already in the spectrum on day 171. The spectrum on day 367 (resolution 5 Å FWHM; Fig. 1, upper panel) shows Hα with the [O I] doublet on its blue side. At later times the Hα profile becomes even more flat–topped, as the [O I] line fades away (P.Meikle, priv. comm.). In an attempt to de–blend the suggested Hα emission, we used a smoothed version of the blue–shifted Mg I] λ4571 line as a template for the two components of the [O I] doublet, and assumed the nebular ratio (1/3). The use of the Mg I] line as a template is justified by the fact that this feature has width and blue–shift similar to those of the oxygen lines (Spyromilio 1994). Of course this template does not include the sub–structures due to clumps, which are clearly detectable in the [O I] doublet profile. Small differences between the profiles of Mg I] and [O I] can affect the resulting de–blended profile, in particular where the flux is low and the S/N ratio worst. This may explain the over–correction visible in Fig. 1 at ∼6250 Å.

After subtracting the [O I] doublet and a symmetric Hα profile obtained from the unblended red half of the line (Fig. 1), the residual is an emission feature, centred at about 6425 Å. The 6425 Å line is also clearly detectable in the spectrum taken on day 171. The identification of this feature is not completely clear. Some Fe II lines (e.g. λ6432 Å of mult. 40) might be possible candidates.

Another narrow bump centred on the rest wavelength of Hα (see Fig. 1) and with FWHM≈ 2000 km s^{-1} is probably also due to Hα. A preliminary conjecture is that this line is of the same nature as the so–called intermediate component of Hα in SN 1988Z, i.e. that it originates from the shocked wind clouds (cf. Chugai & Danziger 1994).

We looked also at the other possible contenders in order to check, if all the 6600 Å band is produced entirely by the Hα emission. We checked the available late time (200–300 days) spectra of SNe Ib/c and found that all of them show an additional emission feature in the red wing of the [O I] doublet, which we tentatively call the '6600 Å feature'. The red edge of this feature extends to about 6800 Å, which corresponds to an Hα radial velocity of ≈ 11000 km s^{-1}. This fact is troublesome, since this value coincides with the red edge of the Hα emission in the late–time spectra of SN 1993J. There is also some indication that another weak emission, near 6150 Å, is present in the blue wing of the [O I] doublet.

From the well observed spectrum of SN 1985F at $t \approx$ 300 days (Filippenko & Sargent 1986) we estimate the luminosity of the 6600 Å emission feature to be ≈ 4 10^{38} ergs s^{-1} (for H_0 = 75 km s^{-1} Mpc^{-1}), which is three times the luminosity of the Hα emission in SN 1993J at the same epoch. However, it should be stressed that the late time luminosity of SN 1985F was particularly high among SNe Ib/c.

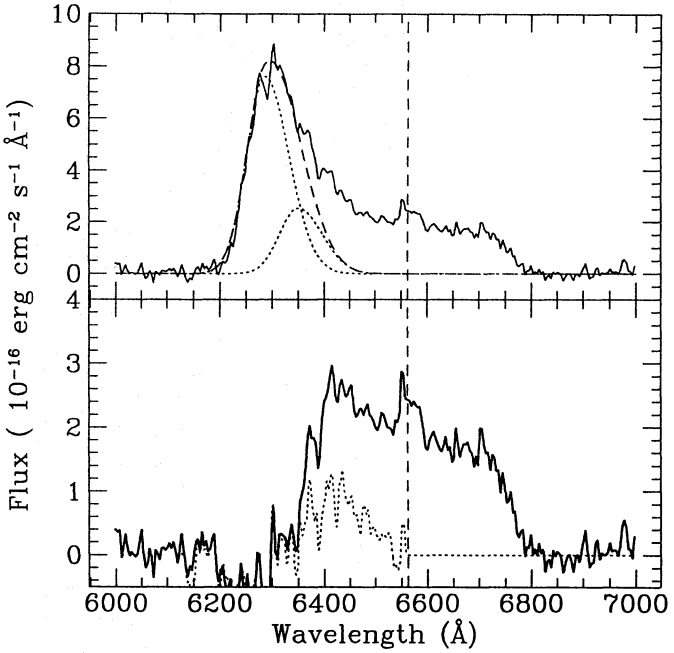

Fig. 1. The spectrum of SN 1993J in the Hα region on day 367. Upper panel: de–blending of Hα at 367 days; the dotted lines are the single components of the [OI] doublet, reconstructed using MgI] λ4571 as a template, while the dashed line is the resulting doublet profile. Lower panel: the same spectrum after subtraction of the [OI] doublet. The dotted line is the residual after subtracting a symmetric Hα profile obtained by reflecting the red wing of Hα around the rest wavelength, indicated by the dashed vertical line

A similar emission feature at the base of [O I] is apparent in the spectrum of the type Ib SN 1983N at 214 days (Gaskell et al. 1986). In this case both the red (6600 Å) band and the blue (6150 Å) band are clearly distinguishable, and have comparable intensities. We thus may hypothesize the presence of a broad blend of emission lines, extending between 6050–6800 Å, underlying the [O I] doublet in the late time spectra of SNe Ib/c. Among the possible candidates are emission lines of Fe II, (cf. QSO spectra, Wills et al. 1985), [Fe II] and possibly [Co II]. The contribution of He I 6678 Å is unlikely to be significant. The intensity of this He I line can be estimated using He I 5876 Å, which is generally a factor ≈ 3.5 stronger than He I 6678 Å (Osterbrock 1989). The straigtforward suggestion is that in all SN Ib/c the 6600 Å feature is simply Hα emission from the remains of hydrogen in the outer layers of SN envelope. However this simple idea faces question, why the spectra close to the maximum light do not offer any support in all SN Ib/c (e.g. SN 1983N) for this identification unlike SN 1993J.

A comparison of SN 1993J and SN 1983N (see Fig. 2) shows that, apart from the overall spectral resemblance, there is a remarkable difference in the ratio of the fluxes of the 6600 Å and the 6150 Å bands, the ratio 6600 Å/6150 Å being much larger in SN 1993J than in SN 1983N. This fact may be regarded as further evidence that Hα emission contributes significantly in the 6600 Å band of SN 1993J. Yet the spectra in Fig. 2 indicate that possibly upto 30% of the emission at the Hα position in

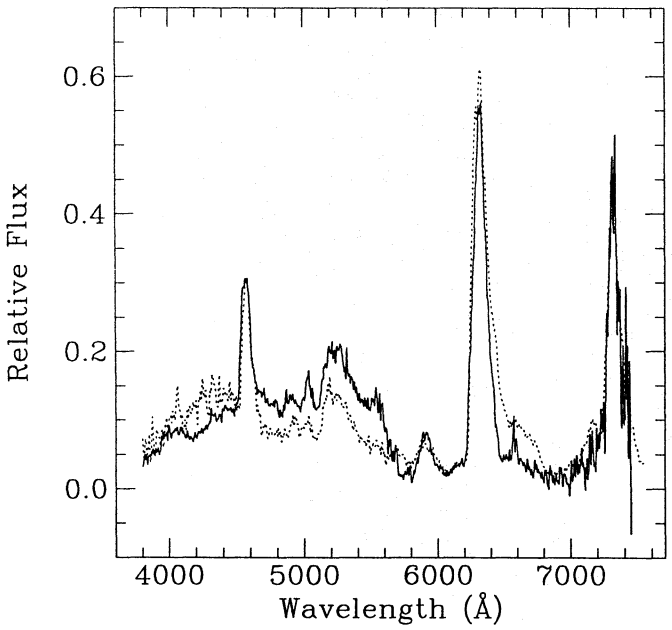

Fig. 2. The spectrum of SN 1983N (Gaskell et al. 1986) on day 214 (thick line) compared to that of SN 1993J on day 255 (dashed line)

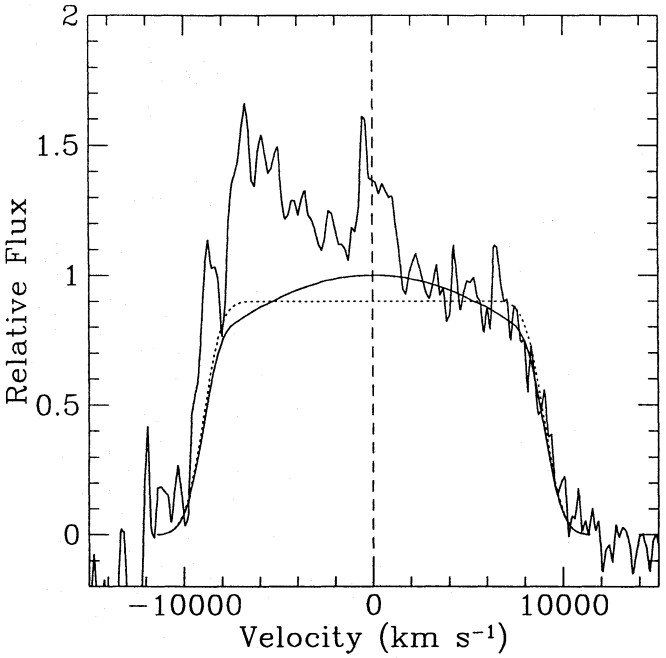

Fig. 3. Best fit to the decomposed Hα profile for day +367. Dashed line: model A, thick line: model B, see text

Table 1. Flux and red edge velocity of Hα. The uncertainty in the figures for the velocity is $\Delta v \sim 400$ km s^{-1}

Date	Phase (days)	Flux (*)	v_e km s^{-1}
15/09/93	171	94.8	11390
19/10/93	205	54.9	11420
19/11/93	236	31.4	11570
08/12/93	255	26.0	11370
21/01/94	299	14.5	11450
30/03/94	367	8.1	11460

(*) Flux in 10^{-14} erg s^{-1} cm^{-2} Å^{-1}.

SN 1993J may originate from the unidentified 6600 Å emission band, which is present in all late–time spectra of SNe Ib/c.

The Hα fluxes (Table 1) were computed as twice the value of the flux measured in the red half of the profile, thus neglecting the possible contribution of the unidentified 6600 Å bump. The Hα flux shows a steady decrease, which is approximately described by $L \propto t^{-3}$ (see Fig. 6). This suggests that the ionization degree remains practically constant during the considered six month period. Another remarkable property of the Hα line is that its red edge velocity at zero intensity, v_e, remains constant within measurement errors during the period 171–367 days (Table 1). This fact imposes important constraints on deceleration effects of the ejecta–wind interaction. Furthermore, the spectrum of SN 1993J obtained at an epoch of 500 days (LPO & RGO database) shows that the edge velocity in the red wing of Hα at zero intensity still did not deviate from the value $v_e \approx 11000$ km s^{-1}.

3. Hydrogen shell

The observed Hα profile can be modelled by some spherically symmetric distribution of the Hα emissivity $j(v)$ in the homologously expanding envelope ($v = r/t$, where t is the expansion time). We consider two possibilities for the emissivity distribution: a one–component model consisting only of a shell of gaussian radial profile with maximum emissivity j_m at a velocity v_m and velocity dispersion σ_m (model A), and a two–component model consisting of the gaussian shell plus an inner zone of constant emissivity j_0 (model B). The choice of a gaussian profile for the shell may seem somewhat questionable, but using more complicated profiles (e.g. a steep increase followed by a plateau and a power law decrease) gives practically the same result, while introducing more free parameters.

Best fits to the spectrum taken on day 367 (Fig. 3) are obtained for models A and B with the emissivity profiles shown in Fig. 4. In the fitting procedure we used only the red wing of Hα, since the blue side is affected by the assumption made in the de–blending process. The edge velocity was fixed at v_e =11400 km s^{-1} (cf. Table 1). The velocity of maximum emissivity, which we will also refer to as the shell position, is v_m = 8900 km s^{-1} in model A and v_m = 9300 km s^{-1} in model B. In both models the velocity dispersion of the emitting shell is σ_m=800 km s^{-1}. Both models reproduce the red part of the Hα profile reasonably well, which means that we cannot rule out the presence of a small amount of hydrogen in the inner region of the envelope ($v < 7500$ km s^{-1}), giving rise to the bump in the emission.

The location of the emissivity maximum is consistent with the radial velocity of the late time Hα absorption (Fig. 4). The

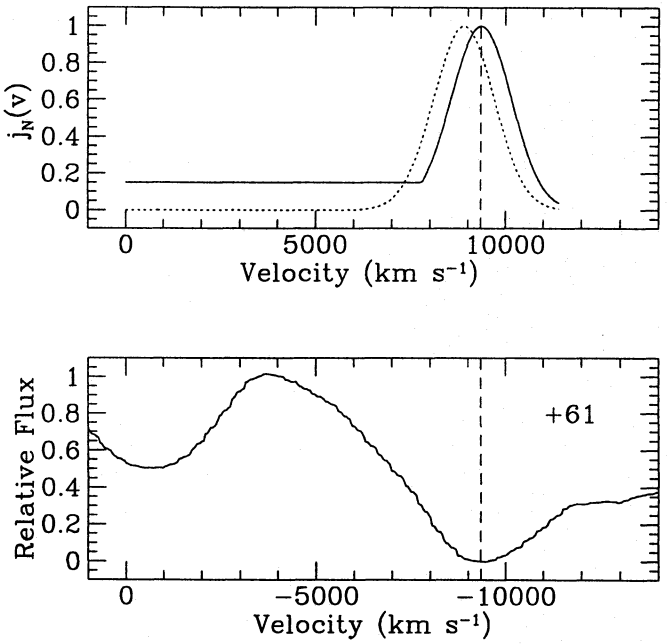

Fig. 4. The emissivity profile of the hydrogen shell. Upper panel: normalized Hα emissivity distribution (dashed line–model A; full line–model B). Lower panel: Hα profile on day 61

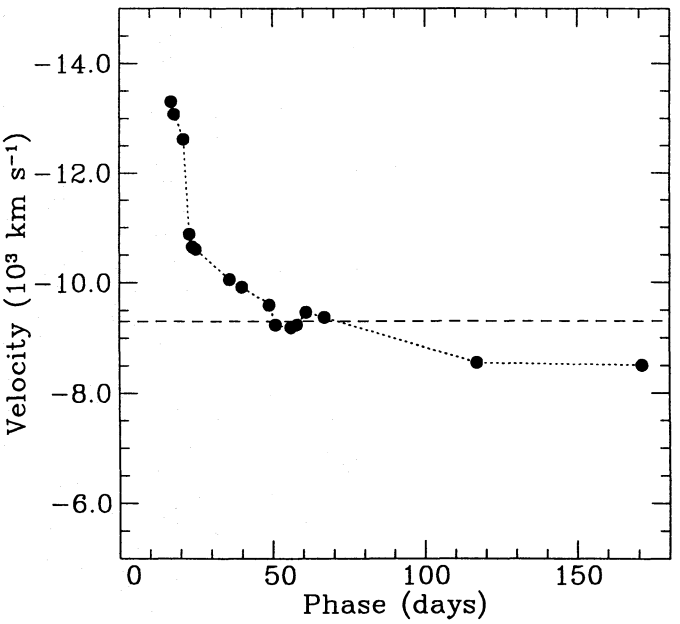

Fig. 5. Evolution of the radial velocity of the absorption minimum in the Hα profile. The horizontal dashed line marks the position of the emitting shell in model B

rapid decline of the radial velocity of the Hα absorption during the first 50 days suddenly stops when the velocity reaches about 9500 km s^{-1}. For at least 20 days thereafter the velocity does not change noticeably (Fig. 5). This behaviour may be understood if one assumes that after day 50 the radius of maximum hydrogen concentration on the second level coincides with that of maximum hydrogen concentration. At later times, after about 100 days, the absorption velocity is slightly lower, 8500 km s^{-1}. This may be caused by the filling–in of the blue part of the Hα absorption by the radiation of the [OI] emission doublet.

4. Mass of ionized hydrogen

Using the Hα emissivity distribution derived above, one can place limits on the mass of the ionized hydrogen. Assuming that recombination is the primary populating process for excited levels, the emissivity of Hα is

$$j = \frac{1}{4\pi}\alpha_{32} h\nu n_e n_{H^+}\,, \qquad (1)$$

where α_{32} is the effective recombination coefficient, which for case B recombination and $T = 10^4$ K is α_{32} =1.14 10^{-13} cm^3 s^{-1} (Osterbrock 1989). Case B is appropriate since the optical depth in Hα at late times for any reasonable model is too small for the branching ratio of the Balmer line photons to be affected. The optical depth effects become noticeable only for $\tau(\mathrm{H}\alpha) > 7$. It should also be emphasized that the scattering of Hα photons is conservative if $\tau(\mathrm{H}\alpha) < 10^4$.

Integrating the emissivity (Fig. 4) over volume, and using Eq.(1), a relation between the mass of the ionized hydrogen and the Hα luminosity can be obtained:

$$M(H^+) = 0.15C\left(\frac{v_e}{11400\,\mathrm{km/s}}\right)^{3/2}\left(\frac{n_{H^+}}{n_e}\right)^{1/2} t_{\mathrm{yr}}^{3/2} L_{38}^{1/2}\, M_\odot\,. \qquad (2)$$

Here C is the structure factor, which is 1 for model A (gaussian shell) and 1.2 for model B (gaussian shell with an inner plateau), t_{yr} is the expansion time in years and L_{38} is the Hα luminosity in 10^{38} erg s^{-1}. Adopting the distance d = 3.6 Mpc, absorption A_V = 0.1 mag (Freedman et al. 1994), and using the flux measured at 367 days, f = 8.1 10^{-14} erg s^{-1} cm^{-2} (Table 1), a value L = 1.26 10^{38} ergs s^{-1} is obtained. Substituting this value in Eq. 2 gives a total ionized hydrogen mass $M(\mathrm{H}^+) = 0.17\,(n_{H^+}/n_e)^{1/2}\,M_\odot$ for model A and $0.2\,(n_{H^+}/n_e)^{1/2}\,M_\odot$ for model B.

Assuming that $n_{H^+} = n_e$, i.e. that the contribution of He electrons is small, an upper limit for the mass of the ionized hydrogen, $M(\mathrm{H}^+) = 0.2\,M_\odot$ is obtained. A lower limit can be found assuming complete H ionization and single ionization of He. In that case $n_{H^+}/n_e \approx 4X/(Y+4X)$, where X is the hydrogen mass abundance and the contribution of metals is neglected. Combining this expression with the derived estimate $M(\mathrm{H}^+) = 0.17\,(n_{H^+}/n_e)^{1/2}\,M_\odot$, we obtain the mass of ionized hydrogen for a given total mass of the H/He envelope at $v > 7500$ km s^{-1}, M_{en}:

$$M(\mathrm{H}^+) = \frac{M_{en}}{6}\left[(1+48X_0)^{1/2} - 1\right], \qquad (3)$$

where $X_0 = (0.17/M_{en})^2$ and M_{en} is expressed in solar masses. Adopting $M_{en} \approx 1.4 M_\odot$ (cf. Utrobin 1993) we derive a lower

limit for the hydrogen mass of $0.07 M_\odot$ and the corresponding hydrogen abundance X =0.05.

Thus, the amount of ionized hydrogen responsible for the observed Hα emission at t = 1 yr is between 0.07 and 0.2 $M_\odot$, provided that the contribution of the other lines apart from Hα in the 6600 Å band is negligibly small. If the unidentified 6600 Å band contributes 50% in the luminosity of the blend, the limits are reduced, correspondingly, to 0.05–0.14 $M_\odot$. The safe range for the amount of the ionized hydrogen is therefore 0.05–0.2 $M_\odot$.

Practically all the ionized hydrogen lies in the narrow shell with average velocity 9000 km s^{-1} and velocity dispersion 800–1100 km s^{-1}, this latter value depending on whether H ($j \propto n_{H^+}^2$) or He ($j \propto n_{H^+}$) is the dominant producer of free electrons. The mass of the ionized hydrogen in the inner region with $v < 7500$ km s^{-1}, as estimated for model B, does not exceed 20% of the total ionized hydrogen mass.

5. Source for Hα luminosity

The ionization in the hydrogen shell of SN 1993J at late times can be produced either by the radioactivity or by the X–rays emitted due to the ejecta–wind interaction. Either of these mechanisms may dominate in SNe II at the age of 1 yr (cf. Chugai 1990). In this section we examine in turn the possibility of each mechanism in explaining the late time Hα emission from SN 1993J.

5.1. Radioactive mechanism

We adopt a simplified model of the supernova envelope: a freely expanding sphere of uniform density and outer boundary velocity v_b, within which hydrogen is uniformly distributed in the range $v_h < v < v_b$, while ^{56}Ni is distributed in the inner zone with $v < v_h$. The model is defined by the following set of parameters: total mass M, kinetic energy E, mass of ^{56}Ni, inner velocity of the hydrogen shell v_h and hydrogen abundance X (the hydrogen shell is assumed to consist of H and He only). In accordance with hydrodynamical models of SN 1993J, we adopt M = 2.4 $M_\odot$, $M_{\rm Ni}$ = 0.075 $M_\odot$and E = 1.44 10^{51} ergs s^{-1}. The value of E follows from the condition $v_b = 10^4$ km s^{-1} and is close to the average of the values given by Woosley et al. (1991), Utrobin (1993) and Shigeyama et al. (1994). We adopt v_h = 7500 km s^{-1}, which corresponds to the inner edge of the hydrogen distribution found from modeling the Hα line in Section 3. The mass of the H/He shell at velocities > 7500 km s^{-1} in our model is 1.4 $M_\odot$, in reasonable accordance with hydrodynamical models. The hydrogen abundance X is then the only free parameter.

The energy from the radioactive decay of ^{56}Ni is deposited into the Hα emitting zone ($v \geq v_h \approx 7500$ km s^{-1}) via the Compton scattering of γ–rays and the subsequent ionization losses of the Compton electrons. Positrons from the electron capture channel, which account for 3.6% of all the decay energy, are slowed down locally in deeper layers and do not contribute to the deposition of energy in the hydrogen shell. Therefore, the total luminosity deposited in the hydrogen layer depends on the absorption of the luminosity of the γ–rays escaping the inner region. Denoting the γ–ray optical depth of the inner region ($v < v_h$) as $\tau_{\gamma,c}$, and that of the hydrogen shell as $\tau_{\gamma,h}$ (the absorption coefficient is $\kappa_\gamma = 0.06\langle Z/A\rangle$ cm^2 g^{-1}), the luminosity deposited in the hydrogen shell may be written approximately as

$$L_{\rm d} = L_{\rm Ni} \frac{1 - \exp(-\tau_{\gamma,h})}{1 + \tau_{\gamma,c}}, \quad (4)$$

where $L_{\rm Ni}$ is the total power released in the ^{56}Ni–^{56}Co –^{56}Fe radioactive decay.

To compute the Hα luminosity we used a one–zone approximation, treating the radiation transfer in the Balmer continuum in terms of the average escape probability (cf. Chugai 1988; 1990). The effective recombination coefficient for Hα varies between case C (very large optical depth in the Balmer lines) close to maximum light, and case B at late time. The dependence of the effective recombination coefficient on the optical depth of the Balmer lines is implemented according to previous prescriptions (cf. Chugai 1990). The dependence of the energy spent in the ionization and excitation of H and He on the ionization degree was modified to include the case when He is a dominant electron producer. The fraction of the energy of the fast electrons spent in the excitation of hydrogen was taken according to the approximation given by Xu et al. (1992). The principal difference between the present radioactive model and earlier versions is the introduction of an inner ^{56}Ni, H–free zone, which results in the dependence of the deposited energy on the optical depth of both zones [Eq. (4)]. This modification affects both the early phase, via the larger deposition of γ–ray energy in the inner zone, and the late–time epoch, due to the absence of positrons in the hydrogen shell.

The evolution of the Hα luminosity resulting from the radioactive model for three values of hydrogen abundance X in the H/He shell: 0.05, 0.2 and 0.7 (i.e. hydrogen mass 0.069, 0.28 and 0.97 $M_\odot$, respectively) is shown in Fig. 6 together with the observed Hα luminosity measured on the Asiago spectra (we adopted D = 3.6 Mpc and A_V = 0.3 mag. from Freedman et al. 1994). It should be emphasized that the model does not take into account the ionization and excitation of hydrogen by the photospheric radiation. Therefore it is applicable only well after the maximum light epoch, i.e. for $t > 40$ days. In any case, at late times the radioactive model appears to produce insufficient luminosity to account for observations after day 120, even for a hydrogen mass as high as 1 $M_\odot$. Assuming that the unidentified emission band at 6600 Å contributes 50% to the Hα emission does not improve the situation markedly: in that case the radioactive model fails after about day 150. At the age t = 1 yr the observed Hα luminosity, 1.3 10^{38} ergs s^{-1}, exceeds the value predicted by the radioactive model with hydrogen mass 0.07–0.3 $M_\odot$ by about one order of magnitude.

The fact that the radioactive mechanism is unable to explain the bulk of the Hα luminosity in SN 1993J at times $t > 150$ days means that some other mechanism must dominate the ionization and excitation of hydrogen. It should be stressed that the effect

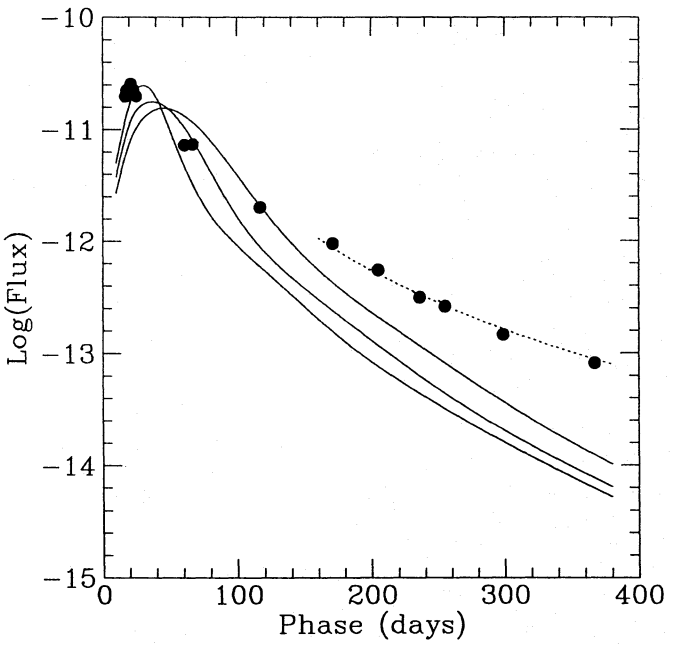

Fig. 6. Hα light curve. The circles are the observed fluxes while the solid lines correspond to the radioactive model (see text) with different hydrogen masses. From bottom to top at late times are models with M_H = 0.069, 0.28 and 0.97 $M_\odot$, respectively. The dotted line reproduces an L$\propto t^{-3}$ decay law

of freezing–out has nothing to do with our result concerning the excess of Hα luminosity over the radioactive model. Actually, even at the age of t = 1 yr the recombination time is still very small compared to the expansion time: $t\,\alpha n_e \approx 7$.

5.2. *Ejecta–wind interaction*

The expansion of the supernova envelope in the smooth CS wind results in a double shock wave structure, with the outer shock propagating in the wind and the reverse shock propagating into the supernova ejecta (for details see: Chevalier 1982a, 1982b; Nadyozhin 1985; Chevalier & Fransson 1994). The shocked gas emits X–rays, dominated by the softer component from the reverse shock. Reprocessing of the X–rays by the outer layers of the ejecta may give rise to the enhanced broad Hα. Depending on whether the reverse shock is adiabatic or radiative, the broad Hα emission originates either from unshocked ejecta ionized by X–rays or from shocked re–ionized cool ejecta. This concept has been applied in particular to the explanation of the strong broad Hα emission in SN 1979C (Fransson 1984; Chevalier & Fransson 1985); SN 1980K (Chugai 1988) and SN 1987F (Chugai 1990). Here the same mechanism is suggested for the Hα luminosity of SN 1993J at $t \geq 0.5$ yr.

In this case, the density in the supernova envelope was assumed to be uniform ($\rho = \rho_0$) in the inner zone with $v < v_0$, and to follow a power law $\rho \propto v^{-\omega}$ in the region $v \geq v_0$. The parameter v_0 is determined given the power law index ω, the mass of the envelope and its kinetic energy. Using the assumed density distribution in the supernova envelope and the wind density $\rho = w(4\pi r^2)^{-1}$, one may write the Chevalier–Nadyozhin self–similar solution for the radius of the ejecta–wind contact discontinuity in the following form:

$$R_s = \left(\frac{6}{\omega(\omega-4)}\frac{M}{w}\right)^{1/(\omega-2)} (v_0 t)^{(\omega-3)/(\omega-2)}. \quad (5)$$

The outer edge of the Hα emitting zone, v_e, may be identified with the contact discontinuity between ejecta and wind material, such that at the phase 0.5–1 yr one has $v_e \approx R_s/t$ = 1.14 10^9 cm s^{-1}. A lower limit for the power law index of the density distribution in the outer layers of the envelope, ω, can be estimated from the absence of any noticeable decrease of the edge velocity v_e between days 171 and 367. With an upper limit for the velocity drop $|\Delta v| \leq 400$ km s^{-1}, Eq. (5) gives a lower limit $\omega \geq 24$, confirming findings from models of the explosion (Shigeyama et al. 1994) and of the photospheric epoch spectra (Baron et al. 1993, Zhang et al. 1994).

Adopting ω=24, M=2.4$M_\odot$ and E=1.4 10^{51} ergs s^{-1}, the velocity parameter of the supernova envelope is v_0=9380 km s^{-1}. From Eq. (5) for t=1 yr and R_s/t=v_e we find then the wind density parameter w=2.8 10^{13} g cm^{-1}, which corresponds to a mass–loss rate $\dot{M}$=4.2 $10^{-7}(u/10$ km s$^{-1})$ $M_\odot$ yr^{-1}, an unexpectedly low value. A larger index ω would lead to an even lower value of the wind density parameter. In fact, this estimate of w depends on the adopted kinetic energy, since $w \propto E^{(\omega-3)/2}$. The maximum energy tolerated by the hydrodynamical models is E = 1.6 10^{51} ergs s^{-1}(cf. Utrobin 1994), which results in the somewhat higher wind density parameter w = 1.1 10^{14} g cm^{-1}, and, correspondingly, in a mass–loss rate 1.7 10^{-6} $M_\odot$ yr^{-1}(for ω = 24 and u_w = 10 km s^{-1}). This must be regarded as an upper limit to the wind density imposed by the dynamical requirements.

In the standard model of the ejecta–wind interaction the broad Hα emission is produced by the reprocessing of the primarily X–ray luminosity of the reverse shock wave, because of the higher emission measure of the shocked ejecta compared with the shocked wind. Assuming that the kinetic luminosity of the reverse shock wave, $L_{k,2}$, converts into Hα luminosity with an efficiency ϕ, we have the following expression for the Hα luminosity:

$$L(\mathrm{H}\alpha) = \frac{1}{2}\phi\frac{L_{k,2}}{L_k} w v_s^3, \quad (6)$$

where $L_k = (1/2)wv_s^3$ is the total kinetic luminosity of the ejecta–wind interaction and v_s is the velocity of the outer shock wave. The ratio of the kinetic luminosities in Eq. (6) is

$$\frac{L_{k,2}}{L_k} \approx \frac{L_{k,2}}{L_{k,1}} = \frac{\omega-4}{2(\omega-3)^2}, \quad (7)$$

(cf. Chevalier 1982b), where we consider $L_{k,1} \approx L_k$, since the luminosity of the inner shock wave is only a small fraction of the kinetic luminosity of the outer shock wave.

The maximum possible efficiency of the conversion of the kinetic luminosity into Hα emission can be estimated as the

probability that the ionization or excitation of hydrogen by the fast electrons produced by the absorption of the X–rays emitted at the reverse shock wave will result in the emission of an Hα photon. This is:

$$\phi \approx \frac{h\nu_{32}}{I_H} \frac{\alpha_{32}}{\alpha_B} p_{i,ex} \approx 0.03, \quad (8)$$

where I_H is the ionization potential of H, $p_{i,ex} = 0.53$ is the fraction of the energy of the fast electrons going into ionization and excitation of levels $n \geq 3$ (Xu et al. 1992), while the ratio of the effective Hα recombination coefficient and the case B recombination coefficient to the excited levels is $\alpha_{32}/\alpha_B = 0.39$.

On day 200, the Hα emission band luminosity is $1.2\,10^{39}$ ergs s^{-1}. If we attribute 50% of this to Hα (the rest is presumably the unidentified 6600 Å emission), we obtain an excess over the radioactive model (with $M_H \leq 0.3\ M_\odot$) of approximately $4.4\,10^{38}$ ergs s^{-1}, which we ascribe to the ejecta–wind interaction mechanism. Using Eqs. (6), (8) and (7), and adopting $\omega = 24$ and $v_s = 10^9$ cm s^{-1} we find then $w = 1.3\,10^{15}$ g cm^{-1}, which corresponds to a wind mass–loss rate $\dot{M} = 2\,10^{-5}(u/10\text{ km s}^{-1})\ M_\odot$ yr^{-1}. This value is at least 10 times greater than the upper limit obtained above from dynamical considerations ($1.7\,10^{-6}\ M_\odot$ yr^{-1}), which means that the standard model of the ejecta–wind interaction faces a serious problem in simultaneously explaining both the high Hα luminosity and the absence of a noticeable decrease of the Hα FWZI.

One way out is to suggest that for some reason, which will be discussed further on, the rate of conversion of the kinetic luminosity of the ejecta–wind interaction into Hα emission is significantly higher than in the standard model, so that even a substantially lower wind density may successfully account for the observed Hα luminosity. As an extreme possibility, one might assume that all the kinetic luminosity L_k is deposited into the internal energy of the ejecta, and that the subsequent conversion into Hα photons proceeds at maximum efficiency [Eq. (8)]. This corresponds to assuming $L_{k,2}/L_k = 1$ in Eq. (6), in which case we obtain the significantly lower wind density parameter $w = 3\,10^{13}$ g cm^{-1}. This value is consistent with the upper limit to the density parameter, $w \approx 10^{14}$ g cm^{-1}, found above from dynamical considerations. However, we must stress that this estimate is only illustrative, and it is not evident that the maximum conversion rate of kinetic luminosity into Hα emission is actually reached.

The primary cause for the more efficient conversion of the kinetic energy into Hα luminosity in the real–life situation of the ejecta–wind interaction, compared with the picture of the standard model, is likely to be the clumpiness of the wind material and, possibly, the clumpy structure of the unstable dense cool shell formed by the reverse shock wave. Basically, clumpiness, i.e. a higher density of the colliding gas, is expected to favour a more efficient transformation of kinetic energy into radiation.

Wind clumpiness was invoked for some supernovae (e.g. SN 1986J, Chugai 1993; SN 1988Z, Chugai & Danziger 1994) to explain the high intensity and the small width of the Hα emission as the result of the emission by the radiative shock wave in dense wind clouds. However, in the case of SN 1993J the narrow Hα emission (FWHM = 2000 km s^{-1}) is relatively weak (if it is present at all), one order of magnitude lower compared to the broad component. This implies certain restrictions on the possible combination of relevant parameters (clump size, density contrast and filling factor), which in principle could be met. In the particular case of SN 1993J wind clumps are needed in order for the kinetic energy of the ejecta–wind interaction to be deposited in deeper layers of the ejecta compared with the case of the smooth wind.

The Rayleigh–Taylor (convective) instability of the cool dense shell formed in the radiative reverse shock is another possible source of clumpiness. The formation of clumpy structures due to this mechanism was addressed in detail by Chevalier & Blondin (1994). They demonstrated that the cool shell is fragmented, producing mushroom–like structures which penetrate the hot gas of the outer shock wave. It might be that the mixture of cool and hot gas produced in this way leads to increasing conversion of the internal energy of the outer shock into Hα luminosity.

Summing up, the ejecta–wind interaction mechanism may account simultaneously for the observed luminosity and width of Hα, and for the absence of deceleration of the H shell, only in the case of a very low average wind density parameter, $w \sim 10^{14}$ g cm^{-1}, which corresponds to a mass–loss rate $\sim 2\,10^{-6}\ M_\odot$ yr^{-1}, and in the assumption of a very high efficiency of the conversion of kinetic luminosity into Hα photons. The clumpiness of the wind and possibly of the shocked ejecta may be responsible for the high Hα photon production efficiency. However, the detailed physical picture of the power supply for the Hα luminosity from the ejecta–wind interaction remains to be understood. Moreover, we leave the open question as to whether such a model could reproduce the observed radio and X–ray emission.

6. Discussion and conclusion

SN 1993J was the first SN Ib ever to show at late time ($t >$ 100 d) a noticeable broad Hα emission line. This is evidently connected with the hydrogen leftovers in the outer layers of the supernova envelope which caused the presence of strong Balmer lines in the photospheric epoch spectra and led to the early type II classification for this object. The unusual strength of Hα close to maximum light compared to other SNe Ib (Ic) showing an Hα line (e.g. SN 1987K, SN 1987M, cf. Filippenko 1988) indicates that the amount of leftover hydrogen in SN 1993J was particularly large for a SN Ib.

Our estimate for the mass of the ionized hydrogen is 0.05–0.2 $M_\odot$. It might well be that H ionization is nearly complete, so that the estimate above corresponds to the actual total hydrogen mass in the envelope. The derived limits for the hydrogen mass are consistent with the hydrodynamical models, which place the total amount of hydrogen in SN 1993J between 0.06 and 0.9$M_\odot$ (Utrobin 1993; Shigeyama et al. 1994; Woosley et al. 1994).

The velocity we obtained for the peak of the hydrogen distribution, 8900–9300 km s^{-1}, is an important characteristic of

the model, since it depends on the explosion energy, the total mass of the ejecta and the hydrogen mass. Therefore, this velocity may be used as an additional restriction for the parameters of hydrodynamical models. As an example, model 13B by Woosley et al. (1994) predicts the position of the peak of the hydrogen distribution to be at 11000 km s^{-1}, which is noticeably higher than our value. In the latest hydrodynamical models for SN 1993J (Utrobin, private communication) the hydrogen peak density actually lies close to 9000 km s^{-1}.

We found that radioactivity fails to account for the Hα luminosity already at $t \geq 150$ days, thus indicating that the ejecta–wind interaction is a dominant energy source for the Hα luminosity as early as at $t \geq 0.5$ yr. The importance of the ejecta–wind interaction as a primary source for the Hα luminosity of SN 1993J at late times ($t > 1$ year) was first suggested by Clocchiatti & Wheeler (1994).

The standard model of the ejecta–wind interaction (smooth power law density distributions in the wind and ejecta with a spherically symmetric contact discontinuity) fails to explain in a self–consistent manner two observed properties of SN 1993J: the high luminosity of the Hα line and the low deceleration of the outer edge of the Hα emitting shell. A model taking into account wind clumpiness and the fragmentation of the cool dense shell might possibly be able to account for a higher rate of transformation of the kinetic energy into Hα luminosity, and thus to satisfy the dynamical requirement for a lower average wind density. The model proposed in this work is, however, too schematic to make quantitative predictions of the radio and X–ray emission to be compared with observations in these bands. Yet it is clear that wind clumpiness must dramatically change the overall picture of the generation of radio and X–ray emission. In this respect, the failure of the standard model of the ejecta–wind interaction to explain the evolution of the radio emission (Weiler et al. 1994) is telling.

The model of a clumpy wind predicts the appearance of an Hα component arising in the shocked wind clumps, provided that the shock wave in the clumps is radiative. Such an Hα component will be narrower than the broad component emitted by the SN ejecta if the density of the gas in the clumps is significantly higher than that of the ejecta. Of this origin are the narrow Hα emission lines observed in SN 1986J, SN 1978K and SN 1988Z (Chugai 1993; Chugai & Danziger 1994). In SN 1993J an Hα emission component with FWHM≈ 2000 km s^{-1} is possibly present (cf. Fig 1). If this is the case then such a feature may tentatively be also identified with the emission from the shocked wind clumps.

It might well be that, apart from the clumpiness, the wind is characterized also by a global non–sphericity. Indication for this comes from the fact that the Hα profile at the epoch of 500 days (LPO & RGO database) reveals a two–horn shape. This type of profile of emission lines was predicted to emerge from the interaction of spherically– symmetric SN with the dense equatorial wind (Chugai & Danziger 1994). A disk–like distribution for the slow wind lost by the progenitor of SN 1993J in its red–supergiant phase is just what is expected if the progenitor was in a close binary system, which is suggested for SN 1993J (see e.g. Podsiadlowski et al. 1993; Woosley et al. 1994) and could be an intrinsic property of SNe Ib/c (cf. Nomoto et al. 1993).

Further observations of Hα in SN 1993J are badly needed, both for the confirmation of the presence of the narrow Hα emission, arising from dense wind clumps and for tracing possible variations in the broad Hα, which might reflect the variation of the mass–loss rate of the pre–SN star.

Acknowledgements. We are indebted to Drs. M. Turatto and E. Cappellaro for making the 30 March 1994 spectrum of SN 1993J available to us. We are grateful to Prof. J. C. Wheeler for allowing us to use the SN 1983N spectrum taken at McDonald Observatory. We are also grateful to Drs. J. Spyromilio and B. Leibundgut for the possibility to read their manuscript, which draw our attention to the two–horn structure of late Hα emission. Finally, the La Palma Observatory & Royal Greenwich Observatory staff are aknowledged for the possibility to access their data by anonymous *ftp*.

This work was conducted as part of the ESO Key–Programme on Supernovae.

References

Barbon, R., Benetti, S., Cappellaro, E., Patat, F., Turatto & Iijima, T., 1994, A&A submitted
Baron, E., Hauschildt, P. H., Branch, D., Wagner, R. M., Austin, S. J., Filippenko, A. V. & Matheson, T., 1993, ApJ 416, L21
Bartunov, O. S., Blinnikov, S. I., Pavlyuk, N. N.& Tsvetkov, D. Yu., 1994, A&A, 281,L53
Chevalier, R., 1982a, ApJ, 258, 790
Chevalier, R., 1982b, ApJ, 259, 302
Chevalier, R.& Fransson, C., 1985, in Bartel, N., ed, Supernovae as Distance Indicators. Springer, Berlin, p. 123
Chevalier, R. & Fransson, C., 1994, ApJ, 420, 268
Chevalier, R.A. & Blondin, J.M., 1994, ApJ (in press)
Chugai, N. N., 1988, Ap&SS, 146, 375
Chugai, N. N., 1990, Sov. Astr. Lett., 16, 457
Chugai, N. N., 1993, ApJ, 414, L101
Chugai, N.N. & Danziger, I.J., 1994, MNRAS, 268, 173
Clocchiatti, A. & Wheeler, J. C., 1994, IAU Circ. n.6005
Cox, D.P. & Tucker, W.H., 1969, ApJ, 157, 1157
Filippenko, A.V., 1988, Proc. Austr. astron. Soc. 7, 540
Filippenko, A.V. & Sargent, W.L.W., 1986, AJ, 91, 691
Filippenko, A. V. & Matheson, T., Ho, L.C., 1993, ApJ 413, L103
Fransson, C., 1984, A&A, 133, 264
Fransson, C., Lundqvist, P. & Chevalier, R., 1994, ApJ (in press)
Freedman, W.L. et al, 1994, ApJ 427, 628
Gaskell, C. M., Cappellaro, E., Dinerstein, H. L., Garnett, D. R., Harkness, R. P. & Wheeler, J. C., 1986, ApJ 306, L77
Nadyozhin, D. K., 1985, Ap&SS, 112, 225
Nomoto K., Suzuki, T., Kumagai, S., Yamaoka, H. & Saio, H., 1993, Nature 364, 507
Osterbrock, D.E., 1989, *Astrophysics of Gaseous Nebulae and Active Galactic Nuclei*, University Science Books, p.80
Podsiadlowski, P. H., Hsu, J. J. L., Joss, P. C., Ross, R. R., 1993, Nature, 364, 509
Ripero, J., Garcia, F. & Rodriguez, D., 1993, IAU Circ., No. 5731
Shigeyama, T., Suzuki, T., Kumagai, S., Nomoto, K., Saio, H. & Yamaoka, H., 1994, ApJ, 420, 341
Spyromilio, J., 1994, MNRAS 266, L61

Swartz, D.A., Clocchiatti, A., Benjamin, R., Lester, D.F. & Wheeler, J.C., 1993, Nature, 365, 232
Utrobin, V., 1994, A&A, 281, L89
Weiler, K., W., Van Dyk, S. D., Sramek, R. A., Panagia, N. & Rupen, M. P., 1994, proceedings of the 34th Herstmonceaux Conference, *Circumstellar Media in the late stages of the stellar evolution*, Cambridge Univ. Press, Cambridge, 1994, p.207
Wills, B.J., Netzer, H. & Wills, D., 1985, ApJ, 288, 94
Woosley, S. E., 1991, in *Tenth Santa Cruz Workshop in Astr. Astrophys.*, ed. S.E. Woosley, Springer Verlag, p.202
Woosley, S. E., Eastman, R. G., Weaver, T.A. & Pinto, P., 1994, ApJ, 429,300
Xu, Y., McCray, R., Oliva, E. & Randich, S., 1992, ApJ, 386, 89
Zhang. Q., Wang, L., Hu, J. Y., Mazzali, P. A., Wang Z. R., 1994, Acta Astrophys. Sinica, in press
Zimmermann, H. U., et al. 1994a, IAU Circ. n. 5748
Zimmermann, H. U., et al. 1994b, Nature, 367, 621

This article was processed by the author using Springer-Verlag LaTeX A&A style file version 3.